Proceedings of the Korean Nuclear Society Autumn Meeting
Seoul, Korea, October 2001

Two-Dimensional Unsteady Conjugate Heat Transfer Analysis of a PWR Pressurizer Surge Line Pipe Subjected to Internally Thermal Stratification

Jong Chull Jo, Yun Il Kim, Sang Jin Cho, Ju Yeop Park, and Sang Jae Kim

Korea Institute of Nuclear Safety
19 Kusung-dong, Yusung-ku, Taejon 305-338, Korea

Abstract

This paper addresses two-dimensional numerical analysis of the unsteady conjugate heat transfer in a PWR pressurizer surge line pipe subjected to internally thermal stratification. The analysis is performed both for the out-surge and in-surge flows in the pressurizer surge line. In the present numerical analyses, the thermally stratified flow in the pipe line during both surge flows are modeled as natural convection for the case where the stratified flow is at a standstill or forced convection for the case where the stratified flow flows slowly enough to be a laminar flow. The finite volume method presented in this paper employs a body-fitted, non-orthogonal grid system to accommodate the pipe wall of circular geometry and the variable interface of the two fluids at different temperatures. This study investigates in detail the effects of surge flow direction, surge flow velocity and interface level of the two thermally stratified fluids on the determination of the transient temperature distributions in the pipe wall. As the result, the circumferential temperature distributions in the pipe wall obtained by changing the interface level of the stratified level are found to be physically plausible. In addition, it is shown that the predictions without taking account of the effects of surge flow direction and velocity can yield less conservative results of the temperature gradients and thermal stresses in the pipe wall. Therefore, it is recommended to take into account the surge flow direction and velocity effects in the analysis for determining reasonably the temperature distributions in the pipe wall subjected to internally stratified flow.

1. Introduction

The integrity of pressurizer surge pipeline at operating pressurized water reactor (PWR) systems is susceptible to be threatened by the thermal stratification causing unacceptable stresses in the pipe wall composing the primary pressure boundary. This led the USNRC to issue its Bulletin 88-11[1], requesting licensees to take proper actions for the resolution of the issue. Hence, the potential thermal stratification in the pressurizer surge line became one of the significant safety concerns of all the country holding PWRs. For addressing this matter, an assessment of the potential for piping damage due to the thermal stratification is needed. Thus, it is very important to determine, as realistic as possible, the transient temperature distribution in the wall of the piping in which thermally stratified flow occurs, as a prerequisite for the assessment.

Several investigators[2-6] have made efforts to determine the temperature distributions in the pipe wall by means of laboratory testing of the particular geometry, measurement of the temperatures on the outer surface of the pipe in the field, or theoretical predictions. There are much difficulties and limitations in applying the first two approaches for operating plants. Only a few literatures addressing the theoretical analyses are available. Smith et al.[2] presented an approximate analytical solution for the steady-state temperature distributions in a pipe wall. Yu et al.[6] obtained temperature distributions for the steady-state heat transfer model of PWR pressurizer surge line which was simplified by using the computer code ANSYS based on the assumptions that the inside of the pipe is exposed to two distinct ambient fluids of which the temperatures are constant. Jung et al.[5] proposed an unsteady two-dimensional natural convection model for the same problem as that considered by Yu et al.[6]. However the grid system used in the numerical calculations was not satisfactory to simulate the initial geometrical condition of the fluid interface. Recently Jo et al.[7] obtained finite volume solutions of the same problem, employing a body-fitted, non-orthogonal grid system to accommodate the pipe wall of circular geometry and the interface of the two fluids at different temperatures, of which the level is variable. However, in those analyses [5-7] the effects of surge flow direction and velocity were not investigated.

This paper addresses two-dimensional numerical analyses of the unsteady conjugate heat transfer in a PWR pressurizer surge line pipe subjected to internally thermal stratification. The analyses are performed both for the out-surge and in-surge flows in the pressurizer surge line. In the present numerical analyses, the thermally stratified flow in the pipe line during both surge flows are modeled as natural convection for the case where the stratified flow is at a standstill or forced convection for the case where the stratified flow flows slowly enough to be a laminar flow

The governing equations are discretized using the finite volume method and the convection term is approximated by a higher-order bounded scheme named as HLPA[8], which is known as a high-resolution and bounded discretization scheme. The method presented in this paper employs a body-fitted, non-orthogonal grid system to accommodate the pipe wall of circular geometry and the interface of the two fluids at different temperatures, of which the level is variable. The cell-centered, non-staggered grid arrangement is adopted and the resulting checkerboard pressure oscillation is prevented by the application of a modified momentum interpolation scheme[7]. The present method employs the SIMPLE algorithm[9] for the pressure and velocity coupling. This study investigates in detail the effects of surge flow direction, surge flow velocity and interface level of the two thermally stratified fluids on the determination of the transient temperature distributions in the pipe wall.

2. Mathematical Formulation

Governing Equations

(a) Two-dimensional natural convection model

Consider a situation that a specified amount of hot fluid flows into a horizontal circular pipe initially filled with cold fluid at the same temperature of the pipe wall, and then occupies the upper position of the pipe suddenly and becomes stationary (see Fig. 1). Consequently this leads to formation of two distinct fluid layers in the pipe. For simplicity, it is assumed that axial conduction through the pipe wall is negligible, the fluids are Newtonian with constant properties, and the Boussinesq approximation is valid. Thus the governing equations of this thermally stratified flow being at a standstill inside the pipe can be expressed in a generalized coordinate system x^j as,

$$\frac{\partial}{\partial x^1}U_1+\frac{\partial}{\partial x^2}U_2=0 \tag{1a}$$

$$\frac{\partial}{\partial t}(J\rho u_1)+\frac{\partial}{\partial x^1}\left[U_1u_1-\frac{\mu}{J}\left\{\frac{\partial u_1}{\partial x^1}D_1^1+\frac{\partial u_1}{\partial x^2}D_2^1+b_1^1w_1^1+b_2^1w_1^2\right\}+Pb_1^1\right]$$
$$+\frac{\partial}{\partial x^2}\left[U_2u_1-\frac{\mu}{J}\left\{\frac{\partial u_1}{\partial x^1}D_1^2+\frac{\partial u_1}{\partial x^2}D_2^2+b_1^2w_1^1+b_2^2w_1^2\right\}+Pb_1^2\right]=\rho g\beta(T-T_{ref})J \tag{2a}$$

$$\frac{\partial}{\partial t}(J\rho u_2)+\frac{\partial}{\partial x^1}\left[U_1u_2-\frac{\mu}{J}\left\{\frac{\partial u_2}{\partial x^1}D_1^1+\frac{\partial u_2}{\partial x^2}D_2^1+b_1^1w_2^1+b_2^1w_2^2\right\}+Pb_2^1\right]$$
$$+\frac{\partial}{\partial x^2}\left[U_2u_2-\frac{\mu}{J}\left\{\frac{\partial u_2}{\partial x^1}D_1^2+\frac{\partial u_2}{\partial x^2}D_2^2+b_1^2w_2^1+b_2^2w_2^2\right\}+Pb_2^2\right]=0 \tag{3a}$$

$$\frac{\partial}{\partial t}(J\rho C_pT)+\frac{\partial}{\partial x^1}\left[U_1C_pT-\frac{k}{J}\left\{\frac{\partial T}{\partial x^1}D_1^1+\frac{\partial T}{\partial x^2}D_2^1\right\}\right]+\frac{\partial}{\partial x^2}\left[U_2C_pT-\frac{k}{J}\left\{\frac{\partial T}{\partial x^1}D_1^2+\frac{\partial T}{\partial x^2}D_2^2\right\}\right]=0 \tag{4a}$$

where

$$U_1=\rho(u_1b_1^1+u_2b_2^1),\quad U_2=\rho(u_1b_1^2+u_2b_2^2),\quad D_m^j=b_k^jb_k^m,\quad w_j^i=\frac{\partial u_i}{\partial x^k}b_j^k$$

and the geometric coefficients b_i^j represent the cofactors of $\partial y^i/\partial x^j$ in the Jacobian matrix of the coordinate transformation $y^i=y^i(x^j)$, J stands for the determinant of the Jacobian matrix and y^i is the Cartesian

coordinate system. In the above equations (1) - (4), ρ, μ, p, k, c_p, β, and g denote respectively density, viscosity, pressure, thermal conductivity, the specific heat, volumetric coefficient of thermal expansion, and the gravitational acceleration. In addition, T_{ref} and u_i are the reference temperature and the Cartesian velocity components in the y^i direction, respectively.

(b) Two-dimensional forced convection model

Consider a situation that hot fluid and cold fluid flow in the PWR pressurizer surge line with a constant bulk velocity. The hot fluid occupies upper portion of the pipe (see Fig. 1). Consequently this leads to the formation of two distinct fluid layers in the pipe. For simplicity, it is assumed in this study that the flow is fully developed and the axial gradients of velocities and temperature are negligible. For simplicity, it is assumed that axial conduction through the pipe wall is negligible, the fluids are Newtonian with constant properties, and the Boussinesq approximation is valid. Thus the governing equation of this thermally stratified flow model can be expressed in a generalized coordinate system x^j as,

$$\frac{\partial}{\partial x^1}U_1+\frac{\partial}{\partial x^2}U_2=0 \tag{1b}$$

$$\frac{\partial}{\partial t}(Ju_1)+\frac{\partial}{\partial x^1}\left[U_1u_1-\frac{1}{\mathrm{Re}\,J}\left\{\frac{\partial u_1}{\partial x^1}D_1^1+\frac{\partial u_1}{\partial x^2}D_2^1+b_1^1w_1^1+b_2^1w_1^2\right\}+Pb_1^1\right]$$
$$+\frac{\partial}{\partial x^2}\left[U_2u_1-\frac{1}{\mathrm{Re}\,J}\left\{\frac{\partial u_1}{\partial x^1}D_1^2+\frac{\partial u_1}{\partial x^2}D_2^2+b_1^2w_1^1+b_2^2w_1^2\right\}+Pb_1^2\right]=\frac{Gr}{\mathrm{Re}^2}TJ \tag{2b}$$

$$\frac{\partial}{\partial t}(Ju_2)+\frac{\partial}{\partial x^1}\left[U_1u_2-\frac{1}{\mathrm{Re}\,J}\left\{\frac{\partial u_2}{\partial x^1}D_1^1+\frac{\partial u_2}{\partial x^2}D_2^1+b_1^1w_2^1+b_2^1w_2^2\right\}+Pb_2^1\right]$$
$$+\frac{\partial}{\partial x^2}\left[U_2u_2-\frac{1}{\mathrm{Re}\,J}\left\{\frac{\partial u_2}{\partial x^1}D_1^2+\frac{\partial u_2}{\partial x^2}D_2^2+b_1^2w_2^1+b_2^2w_2^2\right\}+Pb_2^2\right]=0 \tag{3b}$$

$$\frac{\partial}{\partial t}(JT)+\frac{\partial}{\partial x^1}\left[U_1T-\frac{1}{\mathrm{Re}\,\mathrm{Pr}\,J}\left\{\frac{\partial T}{\partial x^1}D_1^1+\frac{\partial T}{\partial x^2}D_2^1\right\}\right]+\frac{\partial}{\partial x^2}\left[U_2T-\frac{1}{\mathrm{Re}\,\mathrm{Pr}\,J}\left\{\frac{\partial T}{\partial x^1}D_1^2+\frac{\partial T}{\partial x^2}D_2^2\right\}\right]=0 \tag{4b}$$

where

$$\mathrm{Re}=\frac{W_0\,r_i}{\nu},\quad \mathrm{Pr}=\frac{c_p\,\mu}{k},\quad Gr=\frac{g\beta\,r_i^{\,3}(T_h-T_c)}{\nu^2}$$

W_0 is a specified constant bulk velocity of stratified fluid in the x^3 direction, and r_i is the inner radius of the pipe.

Initial and Boundary Conditions

As mentioned previously, the pipe wall is initially at the temperature of cold fluid T_c, and is suddenly exposed to hot fluid at T_h. The initial conditions for this problem are given as

$u_i=0$ ($i=1,2$) in the whole solution domain, $t=0$ (5)

$T=T_c$ in the pipe wall and the cold fluid, $t=0$, for the case of volume out-surge flow model (6)

$T=T_h$ in the pipe wall and the hot fluid, $t=0$, for the case of volume in-surge flow model (7)

where the subscripts c and h stand for cold and hot, respectively.

Because the solution domain is symmetrical thermally and geometrically, only half of the region is needed to analyze. Thus along the symmetry line, the symmetry boundary conditions will be applied for both velocity and temperature. On the solid wall, the velocity of fluid vanishes. For this situation the boundary conditions are

given by

$$u_i = 0\ (i = 1,2) \text{ at the pipe inner surface,} \quad t \rangle 0 \tag{8}$$

$$-k \left.\frac{\partial T}{\partial n}\right|_{x^2} = h(T - T_\infty) \text{ at the pipe outer surface,} \quad t \rangle 0 \tag{9}$$

$$u_2 = 0\ , \frac{\partial u_1}{\partial x^1} = 0\ , \frac{\partial T}{\partial x^1} = 0 \text{ at the symmetry plane,} \quad t \rangle 0 \tag{10}$$

where n is the outward normal to the surface of the wall, T_∞ is the temperature of environment outside the pipe, and h is the heat transfer coefficient.

3. Numerical Method of Solution

Solution Domain Discretization

The sets of governing equations (1) – (4) are solved numerically by a finite volume approach, requiring the discretization of the solution domain into a finite number of quadrilateral control volume cell whose faces are coincided with the non-orthogonal curvilinear coordinate lines. A typical discretized domain is presented in Fig. 2, and also a typical control volume cell is shown in Fig. 3. The values of all computed variables are stored at the geometric center of each control volume cell. The interface between the hot and cold fluids is arranged here to align with a boundary between two rows of cells, i.e. a gridline.

To obtain the curvilinear non-orthogonal mesh shown in Fig. 2, it is assumed that the solution domain is the cross-section of a pair of eccentric cylinders as shown in Fig. 4. The center of the inner solid cylinder is coincided with the intersecting point of the fluid interface and the vertical symmetry line passing the center of the pipe. The outer cylinder is the pipe subjected to internally stratified flow, and the inner cylinder has such a small size of diameter that the effect of its presence on the calculations can be negligible. Thus, the following boundary conditions are applied to the outer surface of the inner solid cylinder with such an infinitesimal diameter.

$$\frac{\partial u_i}{\partial x^2} = 0\ , \quad \frac{\partial T}{\partial x^2} = 0 \ \ (i = 1,\ 2) \text{ at the outer surface of the infinitesimal inner cylinder,} \quad t \rangle 0 \tag{11}$$

Dislocating the inner solid cylinder either downward or upward can easily control the level of the fluid interface with a horizontal straight-line configuration. The grid is generated by using an algebraic method. In this study, the calculations are performed with a grid of 87×72, forming 87 divisions in the circumferential direction and 72 divisions in the radial direction.

Discretization of Governing Equation

The discretization of the governing equations is performed following the finite volume approach, the convection terms are approximated by the HLPA scheme[8], and the unsteady term is treated by the backward differencing scheme. The resulting algebraic equation for a variable φ can be written in the following general form.

$$A_P \varphi_P = A_E \varphi_E + A_W \varphi_W + A_N \varphi_N + A_S \varphi_S + b_\varphi \tag{12}$$

where $A_j\ (j = P,\ E,\ W,\ N\ or\ S)$ are coefficients and b_φ is a source term for variable φ.

Momentum Interpolation Method

For a better resolution of flow field in complex geometries, recently several investigators have developed various calculation methods of momentum equations employing the non-orthogonal, body-fitted coordinates. Among these methods, the non-staggered, momentum interpolation method originally developed by Rhie and Chow[10] is known to be one of the efficient methods and has been widely used because of its simplicity feature of algorithm. In this method, the momentum equations are solved at the cell centered locations using the Cartesian velocity components as dependent variables and the cell face velocities are obtained through the interpolation of the momentum equations for the neighboring cell centered Cartesian velocity components. In the present study, the modified version of the Rhie and Chow's scheme[7, 11] is used to obtain a converged solution of unsteady flows, which is independent of the size of time step and relaxation factors.

Numerical Treatment of Unsteady Conjugate Heat Transfer[12]

For an unsteady two-dimensional conjugate heat transfer problem, the energy equation in a Cartesian coordinate system with temperature as dependent variable can be written as follows:

$$\frac{\partial}{\partial t}(\rho_f C_{P_f} T) + \frac{\partial}{\partial y^j}(\rho_f C_{P_f} u_j T) = \frac{\partial}{\partial y^j}(k_f \frac{\partial T}{\partial y^j}) \quad \text{in the fluid region} \tag{13}$$

$$\frac{\partial}{\partial t}(\rho_s C_{P_s} T) = \frac{\partial}{\partial y^j}(k_s \frac{\partial T}{\partial y^j}) \quad \text{in the solid region} \tag{14}$$

At the fluid-solid interface e, the following continuous heat flux condition is satisfied.

$$-k_f \left.\frac{\partial T}{\partial y^1}\right|_e = -k_s \left.\frac{\partial T}{\partial y^1}\right|_e \tag{15}$$

Following the notations given in Fig. 5, above boundary condition can be rewritten in a discretized form as follows:

$$-k_f \frac{T_e - T_P}{\Delta y_f^1} = -k_s \frac{T_E - T_e}{\Delta y_s^1} \tag{16}$$

Manipulation of above equation gives the value of temperature at the fluid-solid interface.

$$T_e = \frac{1}{\Delta y_s^1 k_f + \Delta y_f^1 k_s}(\Delta y_f^1 k_s T_E + \Delta y_s^1 k_f T_P) \tag{17}$$

A straightforward way of solving the conjugate heat transfer problem is solving Eq. (13) and Eq. (14) separately using the interface temperature T_e as the temperature boundary condition at the fluid-solid interface. However, this practice requires a separate solution of energy equation in solid and fluid regions and the computer program becomes complicated and it is very difficult to implement this practice in a general purpose computer code. To avoid this difficulty, Patankar[9] introduced an equivalent conductivity concept that enables to solve the energy equation in fluid and solid regions simultaneously.

Using the interface temperature given in Eq. (17), the heat flux at the fluid-solid interface can be expressed in terms of T_E and T_P as follows:

$$q_e = -k_e \frac{T_E - T_P}{y_s^1 - y_f^1} \tag{18}$$

where

$$k_e = \frac{k_s k_f}{(1 - f_e)k_f + f_e k_s} \tag{19}$$

$$f_e = \frac{\Delta y_f^1}{\Delta y_s^1 + \Delta y_f^1} \tag{20}$$

We note that the interface conductivity, k_e in Eq. (19), is the harmonic mean of k_f and k_s if the numerical grid is uniform. Since the Eq. (18) is derived from Eq. (15), the continuous heat flux condition is satisfied if we use k_e as the diffusion coefficient for the energy equation at the fluid-solid interface. The physical effectiveness of this equivalent conductivity is well explained in Patankar [9].

By introducing the interface conductivity concept, the energy equations in fluid and solid regions can be solved simultaneously. However, the existence of C_{P_f} and C_{P_s} in the convection and unsteady terms requires a careful programming in solving the energy equation. If we divide C_{P_f} for Eq. (13) and C_{P_s} for Eq. (14) to

avoid this problem and if we introduce the effective diffusivity at the interface as the same way described before, the continuous heat flux condition at the interface will not be satisfied unless C_{P_s} is equal to C_{P_f}. To avoid this problem we divided C_{P_f} for both Eq. (13) and Eq. (14). Then, the continuous heat flux condition at the fluid-solid interface will be satisfied. After some manipulations, the resulting energy equation can be written as follows:

$$\frac{\partial}{\partial t}(\rho_f T) + \frac{\partial}{\partial y^j}(\rho_f u_j T) = \frac{\partial}{\partial y^j}(\frac{\mu_f}{\Pr_f}\frac{\partial T}{\partial y^j}) \qquad \text{in the fluid region} \qquad (21)$$

$$\frac{\partial}{\partial t}(\rho_f \rho_{fact} T) = \frac{\partial}{\partial y^j}(\frac{\mu_f}{\Pr_f}\Gamma_{fact}\frac{\partial T}{\partial y^j}) \qquad \text{in the solid region} \qquad (22)$$

where

$$\rho_{fact} = \left(\frac{\alpha_f}{\alpha_s}\right)\left(\frac{k_s}{k_f}\right), \qquad \Gamma_{fact} = \left(\frac{k_s}{k_f}\right) \qquad (23)$$

We note that the Eq. (21) is the same as the general form of energy equation commonly used in the computational fluid dynamics, especially in the SIMPLE family of solution methods. From above equations we can notice that the only things we have to do in the solution of conjugate heat transfer is the multiplication of ρ_{fact} and Γ_{fact} to the density and diffusion coefficient of fluid respectively in the solid region and the introduction of effective diffusion coefficient at the fluid-solid interface as is done in Eq. (19). To the present author's knowledge this simple and convenient way of treating the unsteady conjugate heat transfer is not reported in the literatures.

When the numerical grid is non-orthogonal, the continuous heat flux condition at the fluid-solid interface can be written as follows:

$$-k_f \nabla T \cdot n = -k_s \nabla T \cdot n \qquad (24)$$

Following the notations given in Fig. 6, the fluid-solid interface conductivity in a generalized grid situation can be derived exactly the same way as is done in the Cartesian coordinate system.

$$k_e = \frac{C_1 C_2 (T_E - T_P) + (C_1 C_4 + C_2 C_3)(T_{ne} - T_{se})}{(C_1 + C_2)[C_5 (T_E - T_P) + C_6 (T_{ne} - T_{se})]} \qquad (25)$$

where

$$C_1 = k_f \frac{(e^1 \cdot n)_f}{\Delta x_f^1}, \quad C_2 = k_s \frac{(e^1 \cdot n)_s}{\Delta x_s^1}, \quad C_3 = k_f \frac{(e^2 \cdot n)_f}{\Delta x_f^2}, \quad C_4 = k_s \frac{(e^2 \cdot n)_s}{\Delta x_s^2}, \quad C_5 = \frac{(e^1 \cdot n)}{\Delta x^1}, \quad C_6 = \frac{(e^2 \cdot n)}{\Delta x^2}$$

$$e^1 = \frac{1}{J}(\frac{\partial y^2}{\partial x^2} i - \frac{\partial y^1}{\partial x^2} j), \; e^2 = \frac{1}{J}(-\frac{\partial y^2}{\partial x^1} i + \frac{\partial y^1}{\partial x^1} j), \; J = \frac{\partial y^1}{\partial x^1}\frac{\partial y^2}{\partial x^2} - \frac{\partial y^1}{\partial x^2}\frac{\partial y^2}{\partial x^1},$$

$$\Delta x^1 = \Delta x_f^1 + \Delta x_s^1, \quad \Delta x^2 = \Delta x_f^2 = \Delta x_s^2$$

We note that the interface conductivity in a generalized grid situation is coupled with the temperature due to the non-orthogonality of numerical grid. However, it does not make any problems since the energy equation is solved iteratively at each time step. The interface conductivity is updated at each iteration level using the newly updated temperature field.

4. Results and Discussion

Based on the present numerical solution method, a computer program for analyzing the thermally stratified flows in horizontal circular pipes was developed. Before applying the computer program to the detailed calculations of practical problems, the natural convection in an eccentric annulus, shown in Fig. 7, experimentally conducted by Kuen and Goldstein[13] was solved to validate the present computer program.

Calculations are performed for Prandtl number 0.7 and Rayleigh number 49,000 employing three different convection schemes. The convection schemes considered in the calculations are HYBRID[9], HLPA[8], and QUICK[14]. Uniform 42×22 numerical grids are employed in the calculations.

Fig. 8 shows the predicted local equivalent conductivity distributions on the cylinder surfaces together with the measured data by Kuen and Goldstein[13]. The local equivalent conductivities are defined as

$$k_{eq} = h_i \, d_i \, \frac{\ln(d_o / d_i)}{2k} \qquad \text{for inner cylinder} \tag{26}$$

$$k_{eq} = h_o \, d_o \, \frac{\ln(d_o / d_i)}{2k} \qquad \text{for outer cylinder} \tag{27}$$

where h_i and h_o are the local heat transfer coefficients at the inner and outer cylinders, respectively.

It is seen from Fig. 8 that the present calculations are in good agreement with the experimental measurements excepting the case where the HYBRID scheme is employed. Fig. 8 shows that the HLPA and QUICK schemes produce nearly the same results that are not distinguishable in the plots. This fact indicates that the HLPA scheme is as accurate as the QUICK scheme while preserving the boundedness of the solution. Our earlier numerical experiments by QUICK scheme produces overshoots and undershoots near the interface between the hot and cold fluid regions. Thus, in the present study, the HLPA scheme is used for all calculations.

The geometry of the surge line and most of the computational parameters used here are the same as those in references[4,5]. In operating reactors, the outer surface of the surge line is insulated with a little heat loss. The overall heat transfer coefficient of $h = 0.79$ W/m^2°C is used in the present analysis. For the case of forced convection model, the surge flow rate of hot or cold fluid in the line coming from or to the pressurizer is considered to be $1.26 \times 10^{-2} \, m^3/\sec$. To investigate the effect of fluid interface level on the temperature distributions in the pipe wall, three different cases were examined. The interface levels for the three cases, respectively, are at heights of $0.25 \, d_i$, $0.5 \, d_i$, and $0.75 \, d_i$ from the horizontal reference line passing through the bottom point of inner wall surface, where d_i is the inner diameter of the surge line.

For simplifying the numerical calculations, the variables of length, time, velocity and temperature appearing in Eqs. (1a)-(4a) are nondimensionalized, respectively, using the reference scales of r_i, $(r_i / g\beta\Delta T)^{1/2}$, $(g\beta\Delta T r_i)^{1/2}$, and $\Delta T = (T_h - T_c)$, while those in the Eqs. (1b)-(4b) are nondimensionalized, respectively, using the reference scales of r_i, r_i / W_0, W_0, and $\Delta T = (T_h - T_c)$, where r_i is the inner radius of the surge line. The dimensionless time step used in the computations is 0.05. The iterative computation for each time step ceases when the maximum of the absolute sum of dimensionless residuals of momentum equations or energy equation, or pressure correction equation is less than 10^{-6}. Relaxation factors of 0.7 and 1.0 were used for momentum equations and energy equation, respectively.

The typical calculation results for both cases of natural convection model ($u_3 = 0$) and forced convection model ($u_3 = W_0$) are presented in Figs. 9-12 to discuss the effects of surge flow and interface level. As an illustration, Fig. 9 presents the variation of the local Nusselt number as a function of the angle at two different elapsed times for the case of out-surging. The average Nusselt number decreases to zero with elapsing of time, and increases with increasing the amount of hot fluid flowing into the pipe section. These are plausible from the fact that the greater the difference in temperature between the fluid and the wall surface, the higher the Nusselt number. It is known that the major effect of thermal stratification in the pressurizer surge line of operating nuclear power plants are displacements, bending, and associated stresses resulting from a significant circumferential temperature difference, which was not considered in the original design. In addition, axial stratification profile affects both the local stresses and the global bending effect at a given pipe cross-section. Therefore, the circumferential temperature difference and distribution as well as their variation along the axial direction of pipe are the most important factors to be examined in the assessment of the piping integrity.

Figs.10 and 11 show the transient maximum circumferential temperature differences both at the inner and outer wall surfaces of the three different cases of fluid interface levels, for the out-surge and in-surge flows, respectively. The calculation results for both the natural and forced convection models are plotted in the figures.

As can be seen in the figures, the maximum value of the temperature difference is higher at the inner wall surface than that at the outer wall surface. It increases to their maximum values at the elapsed dimensionless time zone ranging from 500 to 1800 and then decreases as time elapses further.

The piping section at which the maximum temperature difference is produced is expected to be the case where the fluid interface level is slightly under the height of $0.5 \, d_i$. As shown in the figures, the temperatures decrease

as the interface level increases and the gradients of temperature distributions at the mid-level positions are steeper than at the bottom-level positions.

It is seen from Figs. 10 and 11 that the calculation results of temperature variations (gradients) in the pipe wall in the circumferential direction for the case of $u_3 = 0$ are less significant than for the case of $u_3 = W_0$ when the thermal stratification is evolved by out-surge flow, while those for the case of $u_3 = 0$ are a little more significant than for the case of $u_3 = W_0$ when the thermal stratification is evolved by in-surge flow.

Fig. 12 displays, for the three different fluid interface levels, the calculation results of the transient maximum circumferential temperature differences both at the inner and outer wall surfaces both for the out-surge and in-surge flows with the fluid velocity of $u_3 = W_0$. From this figure, it is found that thermal stratification evolved by the out-surge flow makes the maximum differences in the circumferential temperature both on the inner and outer wall surfaces increases as the fluid interface level decreases below the interface level of 50%, while that by the in-surge flow makes the maximum temperature differences as the fluid interface level increases beyond the interface level of 50%. In addition, it can be re-confirmed from the figures that the temperature on the inner wall surface are much higher than that on the outer wall surface during the early transient time period.

Thus, it is emphasized that the stress analysis using the temperature distributions predicted by neglecting the effects of surge flow direction and velocity can give under- or over-conservative results.

5. Conclusions

Two-dimensional numerical analysis of the unsteady conjugate heat transfer in a PWR pressurizer surge line pipe subjected to internally thermal stratification has been performed for the two cases of out-surge and in-surge flows. For the numerical simulation, a body-fitted non-orthogonal grid system was employed to accommodate the pipe wall of circular geometry and the interface of two fluids at different temperatures of which the level is variable. This study investigated in detail the effects of surge flow direction and velocity in the line and interface level of the two stratified fluids on the determination of the transient temperature distributions in the pipe wall.

It has been shown that the use of temperature distributions predicted without taking account of the effects of surge flow may yield less conservative results in the analysis of thermal stresses in the pressurizer surge line. Therefore, it is recommended to consider the surge flow direction and velocity effects in the analysis for determining the temperature distributions in the pipe wall subjected to internally stratified flow.

References

1. US NRC, "Pressurizer Surge Line Thermal Stratification," NRC Bulletin No. 88-11, 1988.
2. Smith, W.R., Cassell, D. S. and Schlereth, E. P., "A solution for the Temperature Distribution in a Pipe Wall Subjected to Internally Stratified Flow," Proc. of the Joint ASME-ANS Nuclear Power Conf., Myrtle Beach, South Carolina, 1988, pp. 45-50.
3. Talja, A.and Hansjosten, E., "Results of Thermal Stratification Tests in a Horizontal Pipe Line at the HDR-Facility," Nucl. Eng. and Design, Vol. 118, 1990, pp.29-41.
4. Ensel, C., Colas, A. and Barthez, M., "Stress Analysis of a 900 MW Pressurizer Surge Line Including Stratification Effects," Nucl. Eng. and Design, Vol 153, 1995, pp.197-203.
5. Jung, I.S., et al., "Thermal Stratification in a Horizontal Pipe of Pressurizer Surge Line," Transactions of KSME; Part B, Vol.20, No.4, 1996, pp.1449-1457.
6. Yu, Y.J., et al., "Structural Evaluation of Thermal Stratification for PWR Surge Line," Nucl. Eng. and Design, Vol.178, 1997, pp.211-220.
7. Jo, J. C., Kim, Y. I., and Choi, S. K., "Numerical Analysis of Thermally Stratified Flow in a Circular Pipe Line," ASME PVP-Vol. 396, Emerging Technologies in Fluids, Structures, and Fluid/Structure Interactions, 1999, pp. 33-39.
8. Choi, S. K., Nam, H. Y. and Cho, M., "Evaluation of a Higher- Order Bounded Scheme: Three- Dimensional Numerical Experiments," Numerical Heat Transfer, Part B, Vol. 28, 1995, pp. 23-28.
9. Patankar, S. V., Numerical Heat Transfer and Fluid Flow, McGraw-Hill, New York, 1980.
10. Rhie, C. M. and Chow, W. L., "Numerical Study of the Turbulent Flow Past an Airfoil with Trailing Edge Separation," AIAA J., Vol. 21, No. 11, 1983, pp.1525-1532.
11. Jo, J. C., Kim, Y. I., Shin, W. K., and Choi, S. K., "Three-Dimensional Numerical Analysis of Thermally Stratified Flow in a Curved Piping System," ASME PVP-Vol. 414-1, Emerging Technologies in Fluids, Structures, and Fluid/Structure Interactions, pp. 31-47, 2000.
12. Jo, J. C., Kim, Y. I., Kim, W. K., Cho, S. J., and Choi, S. K., "Numerical Analysis of Unsteady Conjugate Heat Transfer for Initial Evolution of Thermal Stratification in a Curved Pipe," Proceedings of the KNS

Autumn Annual Meeting, Taejon, Korea, October 2000.
13. Kuehn, T. H. and Goldstein, R. J., "An Experimental Study of Natural Convection in Concentric and Eccentric Horizontal Cylindrical Annuli," J. of Heat Transfer, Vol. 100, pp.635-640, 1978.
14. Leonard, B. P., "A Stable and Accurate Convective Modeling Procedure Based on Qudratic Interpolation," Compt. Methods Appl. Mech. Engrg., Vol. 19, pp. 59-98, 1979.

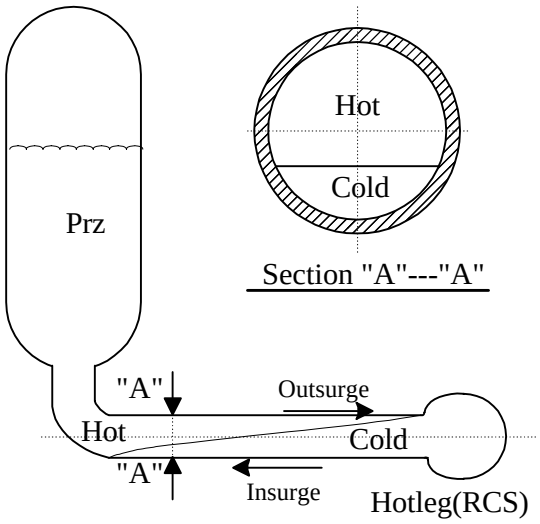

Fig. 1 Thermally stratified flow in a circular pipe.

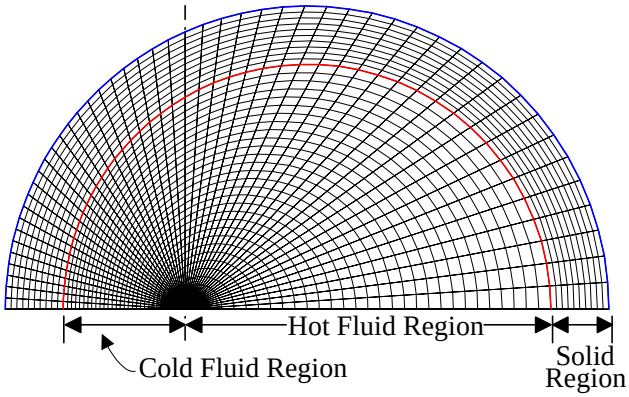

Fig. 2 The curvilinear non-orthogonal mesh.

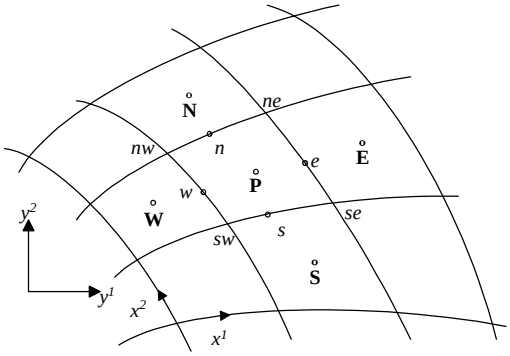

Fig. 3 A typical control volume cell in the computing mesh.

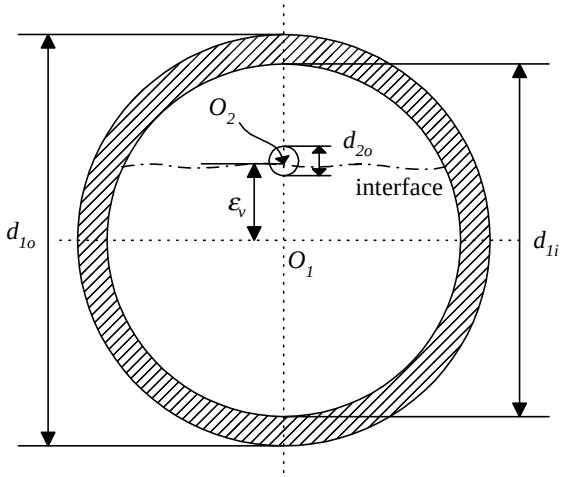

Fig. 4 The imaginary eccentric cylinder for mesh generation.

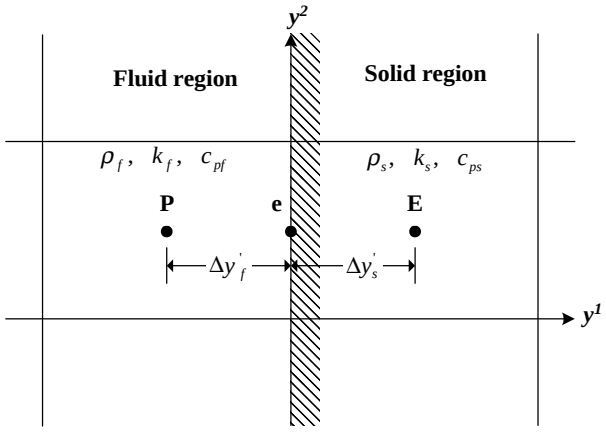

Fig. 5 Fluid-solid interface in an orthogonal grid.

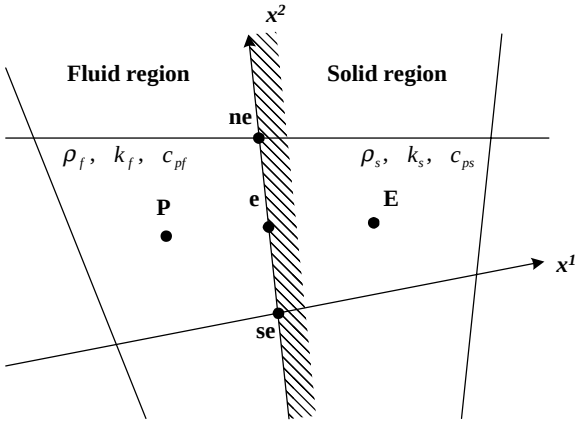

Fig. 6 Fluid-solid interface in a non-orthogonal grid.

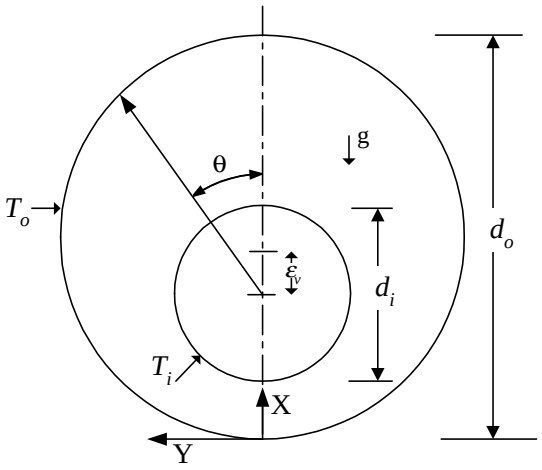

Fig. 7 The annulus between two eccentric cylinders.

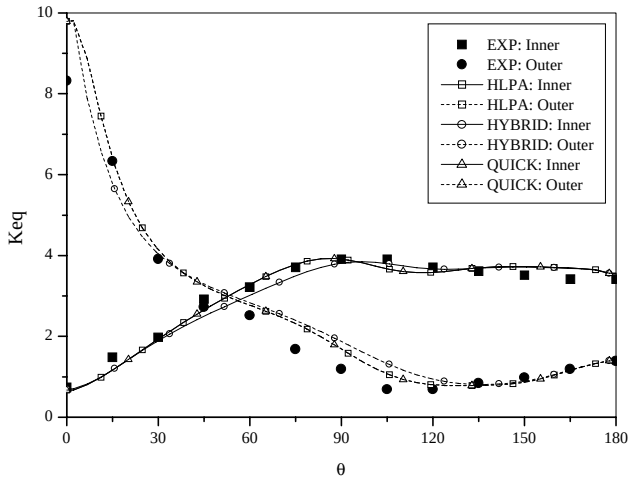

Fig. 8 Comparisons of local equivalent conductivity distributions calculated by the present computer program with experimental measurements[13].

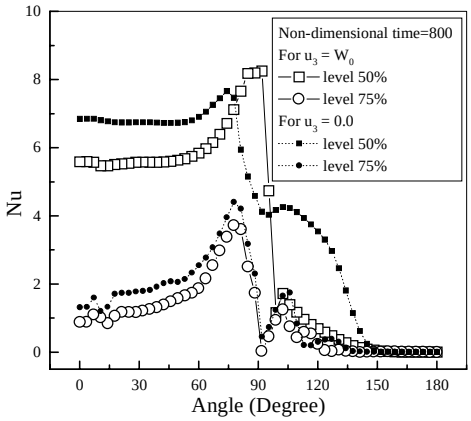

(a) Non-dimensional time = 800

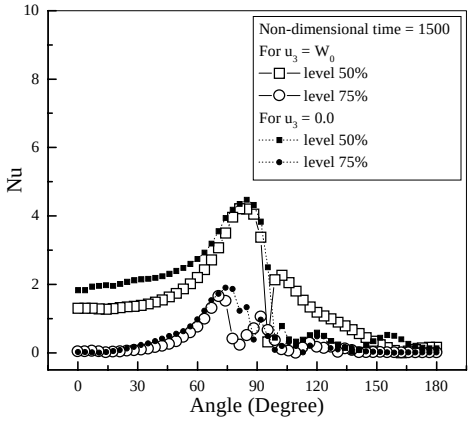

(b) Non-dimensional time = 1500

Fig. 9 The variation of the local Nusselt number(Nu).

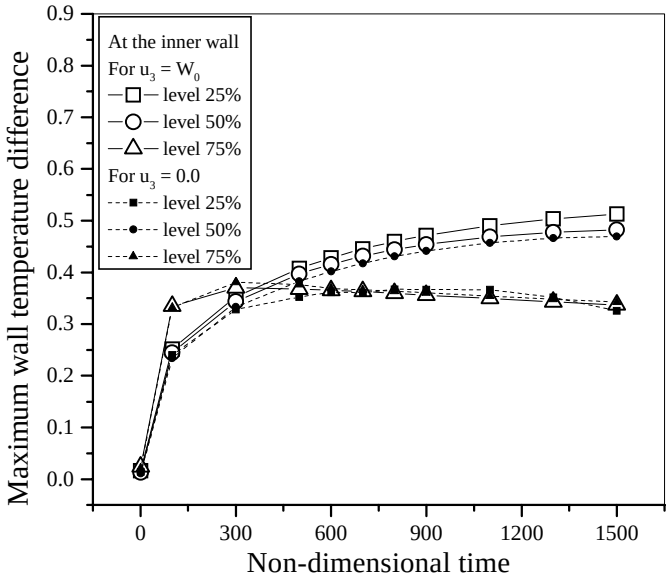

(a) On the inner wall

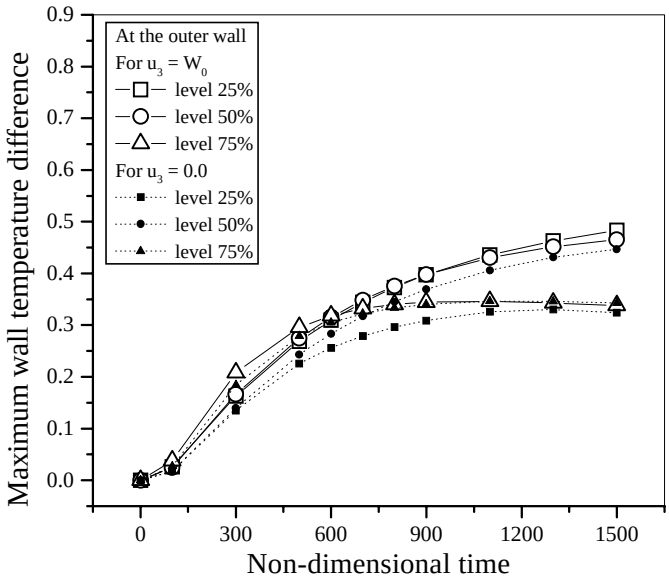

(b) On the outer wall

Fig. 10 Transient maximum wall temperature differences both on the inner and outer wall surfaces.

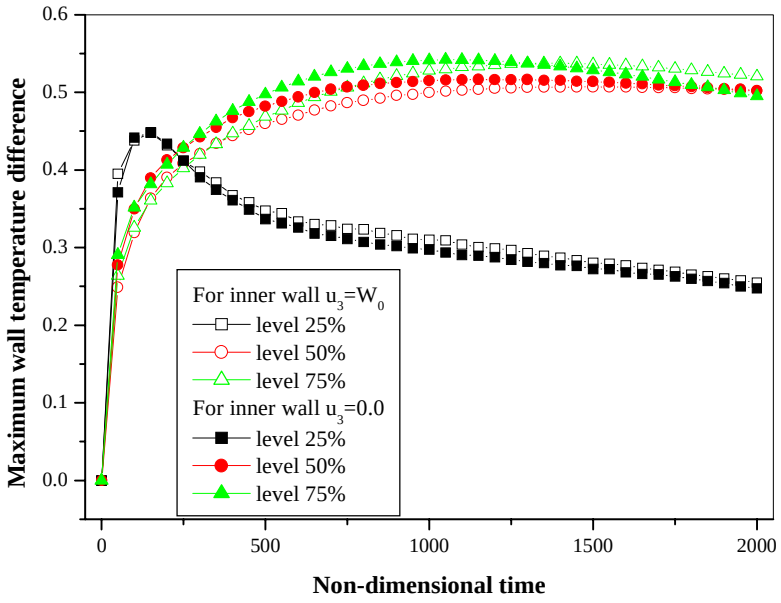

(a) For the inner wall

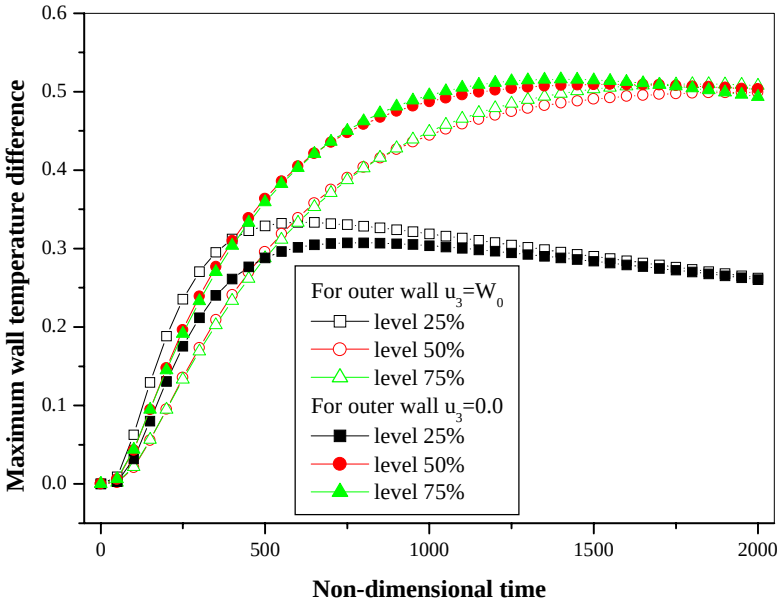

(b) For the outer wall

Fig. 11 Transient maximum wall temperature differences both on the inner and outer wall surfaces for the case of in-surge flow.

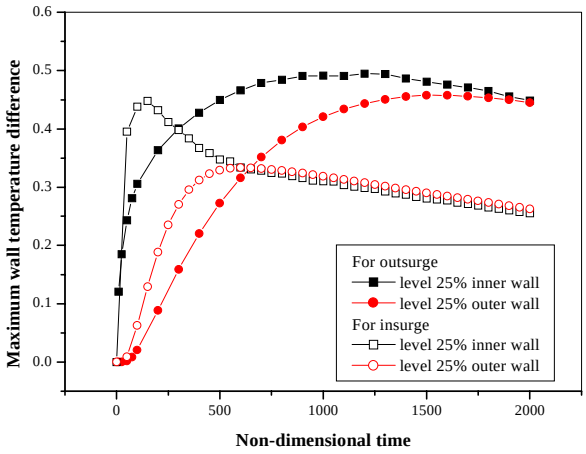

(a) For the interface level of 25%

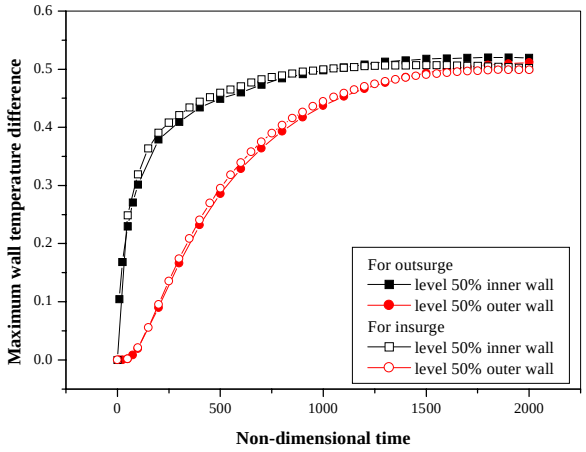

(b) For the interface level of 50%

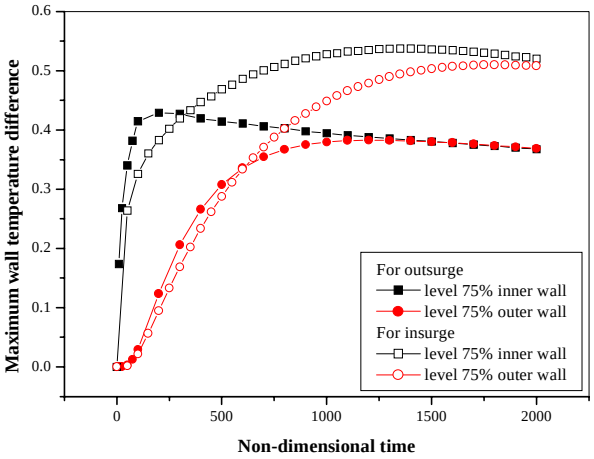

(c) For the interface level of 75%

Fig. 12 Transient maximum wall temperature differences on the outer and inner wall surfaces both for the cases of out-surge and in-surge flows with the axial velocity $u_3 = W_0$.